Preparation of printable and biodegradable cellulose-laponite composite for electronic device application

Saravanan Chandrasekaran,*[a,d] Maria Sotenko,[b] Alvaro Cruz-Izquierdo,[a] Zuhayr Rymansaib,[c] Pejman Iravani[c], Kerry Kirwan[b] and Janet L Scott*[a]

[a]Centre for Sustainable Chemical Technologies and Department of Chemistry, University of Bath, Claverton Down, Bath, BA2 7AY, United Kingdom

[b]Warwick Manufacturing Group, International Manufacturing Centre, University of Warwick, Gibbet Hill, Coventry, CV4 7AL, United Kingdom

[c]Department of Mechanical Engineering, University of Bath, Claverton Down, Bath, BA2 7AY, United Kingdom

[d]Department of Chemistry, School of Engineering, Presidency University, Rajanukunte, Itgalpura, Bangalore – 560064, India.

Email: j.l.scott@bath.ac.uk
Saravanan.chempoly@gmail.com

Abstract:

Printable and biodegradable printed circuit boards (PCBs) prepared by using cellulose as the continuous matrix, laponite as flame retardant filler with various weight ratio (0, 5, 10 and 20 wt% with respect to the α-cellulose quantity used to prepare the composites) and 1-ethyl-3-methylimidazolium acetate ([emim][OAc]) as the recoverable dissolution medium. Prepared cellulose-composites were subjected into physical, chemical, thermal, mechanical and biodegradation analyses to check the suitability of the cellulose-laponite composite for biodegradable electronic application. The addition of laponite into cellulose increased the degradation temperature, flame retardancy and decreased the mechanical properties of the cellulose-laponite composites. The surface nature of the cellulose composite converted from hydrophilic to hydrophobic creased (contact angle value increased in the range from 50° to 112°) by treating with relatively small amount of hydrophobizing agent (< 1wt%). The conductive ink printing experiments on the composites explaining the role hydrophobizing agent and laponite in the composites. Biodegradability of the cellulose was evaluated by enzyme treatments and derived the effect of laponite, hydrophobic agent and conductive ink.

Keywords: α-cellulose; laponite clay; ionic liquid; hydrophobic agent; biodegradable electronics.

1. Introduction:

Printed circuit boards (PCBs) is the main functional unit in the electronic products including laptops, smartphones, television, tablets, etc and PCBs are consists with several metals (~40%), polymers (~30%) and ceramic materials (~30%). At the end of the use, recovering the valuable metals from the used electronic waste products is directly related to the environmental and economic impacts. Existing PCBs substrate materials are made from non-degradable materials such as glass, polyimide, polyethylene terephthalate, polyethylene naphthalate, polycarbonate, etc. Therefore, design of modern electronic products with degradable or depolymerisable PCBs is increasingly important to recover and reuse the materials from e-waste at the end of the lifecycle of electronic goods.

Green electronics is an emerging area of research aimed at finding compounds from natural and renewable resources for the production of materials that have applicability in biodegradable and biocompatible devices. While designing new PCB materials with "Green Electronics" concept the following fundamental points needs to be considered to meet the similar performance and overcome the existing problems in the traditional PCBs, (i) starting materials must be highly available from renewable resources, (ii) economically feasible and low cost processing routes, (iii) do not generate toxic waste, (iv) high flame retardant property against flame, (v) mechanically robust and (vi) easily biodegradable in presence of enzyme (or) in soil.

Cellulose is the most abundant biomass material in nature, available from renewable resources and possesses some promising properties, such as high availability, mechanical robustness, biocompatibility, biodegradability combined with non-toxic degradation products and easiness with which surfaces can be readily chemically functionalized. The above attractive properties make cellulose based materials being widely used in many fields such as paper industry, textile, packaging, absorbents, electronics, biosensors, pharmaceutical industries, energy storage devices and biofuel production [1–12]. Despite the aforementioned beneficial properties of the cellulose, it's insoluble in most of the organic solvents, flammable and the surface of the cellulose is hydrophilic nature Therefore, fulfilling all the above criteria (i-vi) remains truly challenging. Thus, there is a need for new solvents capable to dissolve cellulose for its further processing, flame retardant fillers are required to increase the flame retardancy properties and surface functionalization is required to convert the cellulose surface from hydrophilic to hydrophobic which will be more suitable for printing conductive circuits on the surface of the substrate. Recently, several researchers utilized ionic liquids (ILs) as the

environmental friendly solvent to dissolve the cellulose and they found that ILs is the best dissolution medium [13–21]. In this work, cellulose-laponite composite materials were prepared by using 1-ethyl-3-methylimidazolium acetate ([emim][OAc]) as the recoverable dissolution medium, laponite clay as the inorganic fillers to improve the thermal stability and the flame retardancy and ethyl 2-cyanoacrylate (E2CA) as the hydrophobic agent.

The conductive ink printing studies were carried out on the prepared non-hydrophobized and hydrophobized cellulose-laponite composites we derived the effect of laponite and hydrophobic agent on the printability of the cellulose composites. Moreover, a biodegradability study was carried out on all the samples including the conductive ink printed cellulose composite materials in the presence of a commercial cocktail of cellulases (EC 3.2.1.4). We found the effect of laponite clay, conductive ink and polyethylcyanoacrylate on the biodegradability of the cellulose.

2. Experimental details:

Materials: α-cellulose (Sigma) was dried under vacuum (rota-vapor) for 4 hrs at 80°C, 1-ethyl-3-methylimidazolium acetate ([emim][OAc]) (BASF, Basionics, > 95 wt%) was kept under vacuum (Schlenk line) for 4 hrs at 90°C. HPLC grade methanol, acetone and toluene (Sigma-Aldrich) as well as ethyl 2-cyanoacrylate (Aldrich) are used as received. Laponite RD (hydrous sodium lithium magnesium silicate, $[Mg_{5.5}Li_{0.3}Si_8O_{20}(OH)_4]Na_{0.7}$) with the size of ~25 nm diameter by ~1 nm thickness (from www.byk.com website technical brochures details, pdf file name LAPONITE-Performance Additives) is received as a gift sample from BYK-Chemie GmbH, Germany (Former Rockwood additives) and the laponite was kept under vacuum for 4hrs at 100°C to obtain a free flow white powder. Crystalline silver acetate ($C_2H_3AgO_2$, anhydrous, 99%) was purchased from Alfa Aesar. Ammonium hydroxide (Certified AR, 25% assay) and formic acid (90%, extra pure, SLR) were purchased from Fisher Scientific and 1,4-butanediol (Reagent Plus, 99%) was purchased from Sigma. Celluclast 1.5L® produced by *Tricoderma reesei* ATCC 26921, citric acid monohydrate, 3,5-dinitrosalicylic acid (DNS), sodium hydroxide, sodium potassium tartrate, phenol and sodium metabisulphite were obtained from Sigma-Aldrich. All chemicals were used without further purification.

Preparation of cellulose-laponite composite film:

In this work the Brabender plastograph (BP, GmbH & Co. KG, Germany) was used as the mixer to prepare the cellulose-laponite composites in the presence of [emim][OAc] as the dissolution medium. Hereafter, BP called mixer is mentioned in the entire manuscript. The mixer was pre-heated to 90°C and the blade rotation speed was set to 70 rpm. In a typical experiment, Cellulose composite with 20 wt% laponite was prepared as follows: 68 g of [emim][OAc] (85wt% w.r.t the total weight of cellulose and [emim][OAc]) was added into the pre-heated mixer and 12 g of α-cellulose (15 wt% w.r.t the total weight of cellulose and [emim][OAc]) was divided into 4 x 3 g and added into the mixer consecutively for every 5-mins. Then, 3 g of laponite (20 wt% w.r.t the amount of α-cellulose used in the dissolution process) was added into the dissolved α-cellulose at 20^{th} mins and mixed for another 10 mins at 90 °C. The resultant highly viscous yellowish cellulose-laponite composite was collected from the mixer and kept in an air-tight container for further processing.

The composite material was kept in-between the bake-o-glide sheets (bake-o-glide is a non-stick baking sheet which is polytetrafluoroethylene (PTFE) - coated fabric) and pressed in the metal press for 3 hrs under vacuum at 90°C. [emim][OAc] is completely soluble in methanol solvent. Therefore, the obtained composite film was kept in pure methanol bath and

the bake-o-glide sheet was peeled-off from the cellulose composite to regenerate the composite from [emim][OAc]. [emim][OAc] in methanol solvent was recovered by removing the methanol in the rotary evaporator. The obtained film was kept in between the porous plates and dried under room temperature for 24 hrs. The recovered [emim][OAc] was analysed by ^{1}H NMR spectroscopy and we found that there was no structural changes during the dissolution process.

^{1}H NMR of recovered [emim][OAc]: 400 MHz, D_2O, δ/ppm 1.42 (t, *J*=7.37 Hz, 3H, $NCH_2\mathit{CH_3}$), 1.82 (s, 3H, $\mathit{CH_3}COO^-$), 3.81 (s, 3H, $N\mathit{CH_3}$), 4.15 (q, *J*=7.34 Hz, 2H, $N\mathit{CH_2}CH_3$), 7.34-7.41 (d, 2H, imidazole ring, N*CHCH*N) and 8.63 (s, 1H, imidazole ring, N*CH*N).

Characterization of Cellulose-laponite composites:

Attenuated total reflectance-Fourier transform infrared spectroscopy (PerkinElmer, ATR-FTIR) was recorded in the frequency range from of 4000 cm^{-1} to 600 cm^{-1}. The thermal oxidative degradation stability of the regenerated cellulose and their composites with laponite was analysed by thermogravimetric analysis (SETARAM instruments, TGA 92) under air atmosphere at the heating rate of 5°C/min. The prepared composites along with the native α-cellulose and laponite powders were analyzed by X-ray diffraction (XRD). X-ray diffraction analysis was carried out using PANalytical Empyrean X-Ray Diffractometer with CoKα radiation at 45 kV and 40 mA at a range of 2θ = 5-90° with a step of 0.7°/min. A line focus and spinning stage modes were utilized for the analysis. ^{1}H NMR spectra (in D_2O) of the purified and recovered [emim][OAc] were recorded on a Bruker Avance 400 MHz Spectrometer. Chemical shift of NMR are given in ppm downfield from TMS. Contact angle (CA) measurements were made using the sessile droplet method in air at room temperature with 5 µL droplets of di-ionized (DI) water as the solvent. The composite was then placed on the goniometer and still images were obtained using a Discovery VMS-001 USB microscope (Veho). The subsequent images were used to calculate the contact angle of the droplet, utilizing Dropsnake software with the ImageJ imaging process package. Each data point is an average of 12 measurements within the error ±2°. Surface topography measurements on non-hydrophobized and hydrophobized cellulose with 0% laponite were made using Veeco MultiMode atomic force microscopy (AFM) with a NanoScope IIIa controller. AFM images were used to calculate the Roughness Average (Ra), Root Mean Square (RMS) roughness and other details using Gwyddion software. The average particle size of laponite was analysed by Scanning electron microscopy (JEOL SEM6480LV microscope) and the values were calculated using imageJ software.

The tensile tests were carried out on dog bone-shaped samples with a middle section of 35 mm in length, 9 mm in width and 0.4 mm in thickness using a Static 30 kN Instron which is equipped with Bluehill software and the analysis was carried out with a ramp rate of 2.00 mm min^{-1} at room temperature and a humidity of 40 %. Usually, 7-9 samples were tested and the standard deviation was calculated.

The fractured cross-sections of the samples obtained after the tensile tests were studied with the Scanning Electron Microscopy (SEM). The samples were mounted on the SEM sample holders using a carbon tape and silver paint was applied to the boundary between the lower part of the samples and the holder in order to reduce the charging of the samples. After drying the samples were double coated with gold using an auto sputter coater, Agar Auto Sputter Coater, Stanstead, UK. The SEM micrographs of the composites were obtained using a Zeiss Sigma microscope, Carl Zeiss Ltd., Welwyn Garden City, UK. The working distance ranged between 4-8 mm, the voltage applied was 5-15 kV and both inlens (InLens) and second electrons (SE2) modes were used to obtain images.

Flame retardancy (FR) test on Cellulose-laponite composites:

In this research work, we did not follow any standard FR test procedure. Instead, FR test was carried out on the cellulose-laponite composite films using the following simple method: a cellulose-composite sample (length 5.5 to 7 cm, width ~ 1.2 cm and thickness 0.14-0.23 mm) was held in the clamps in a vertical direction and the flame, ignited by the gas lighter, was directed towards the edge of the film allowing the material to be burned. The flame retardancy was assessed based on the difference between the initial length of the cellulose film and the remaining length after being subjected to the FR test and burned under the fire for 16 seconds. The experiment was repeated three times and an average value was reported. The following formula was used to calculate the % of burned materials:

$$\%\ \text{of the burned material} = \frac{\text{length of the composite before the FR test} - \text{length of the composite after the FR test}}{\text{length of the composite before the FR test}}$$

Hydrophobic coating on Cellulose-laponite composites:

The procedure for the preparation of hydrophobic composites consists of spreading the ethyl 2-cyanoacrylate on the surface by immersing the composites in the pre-prepared solution containing 0.2 g (1 wt%) of E2CA in 19.8 g of toluene solution for 1 hr at 4°C. As the polymerization can be initiated by moisture present in the atmosphere, the composite materials

were kept under the lab atmosphere for 1 hr to initiate the polymerization of E2CA to polyethyl cyanoacrylate (PECA) on the surface of the composites. The same procedure was repeated for another round of coating to make sure the surface of the cellulose-composite coated completely with PECA. The resultant surface modified composites were subjected to further characterization studies.

Experimental procedure for conductive ink printing on the cellulose-laponite composites:

Conductive Ag-ink was prepared by the following method: 1 g silver acetate was dissolved in 2.5 mL of aqueous ammonium hydroxide at room temperature for 15 seconds, followed by the addition of 0.2 mL formic acid, mixing for a further 2 minutes with a magnetic stirrer, conditioning of the mixture overnight and final filtration with a 200 nm syringe filter. The ink was modified by addition of 10% vol 1,4 -butanediol as a viscosifying aid to promote good jetting.

Conductive ink printing on the cellulose composites was carried out on a custom built 3D printer controlled via a LabVIEW program. The cellulose samples were imaged on a Leica M205C equipped with a DFC425 camera unit. The printer was equipped with a 50 μm orifice piezo inkjet nozzle (Microfab MJ-ABP-01-50-8MX) controlled via accompanying JetDrive III unit. This is set up with a custom waveform. The printer was set up to print three parallel lines at different drop densities on the samples at a speed of 3 mm/s. The drop densities are 5, 10 and 15 drops/mm. Distance between the nozzle and material surface (standoff distance) was set at 2mm. Printing is performed on both sides of samples from a given batch. The waveform used is an asymmetric square wave; the initial positive pulse has amplitude of 17V with duration of 9 μs, the negative pulse (echo) amplitude of 15V for 12μs. The cellulose-composite are then sintered on a hot plate at 50 °C for 10 mins to render the tracks visible for evaluation, given the nature of the ink used; at this temperature silver nanoparticles precipitate out of the solution and give an orange/brown stain on the substrate. These experiments were used to evaluate how the hydrophobic treatments and whether addition of filler to the cellulose affected droplet and line formation on the cellulose samples, and thus provide insight on whether highly conductive tracks can be produced.

Enzymatic hydrolysis tests on Cellulose-laponite composites:

A typical enzymatic hydrolysis experiment was based on incubating 3 mg of composite film sample (with the thickness of ~100 μm) in 0.2 mL of sodium citrate buffer (50 mM, pH 5.0) with Celluclast 1.5L® (1 Filter Paper Unit/g of sample) for 1h at 50 ˚C. All reactions were run in triplicates. The cellulose degradation/hydrolysis due to enzymatic activity of Celluclast

1.5L® was determined by measuring soluble reducing sugars via DNS assay [22]. PECA coated on the surface of the cellulose-composites are soluble in acetone solvent. Therefore, biodegradable activities were measured before and after the acetone wash by immersing samples in 5 mL acetone for 1h at RT, and further evaporation of acetone via samples drying on air.

3. Results and discussion:

Prepared cellulose-laponite composites were characterised by physical, chemical, thermal and biodegradable studies to check the suitability of the cellulose composites for biodegradable printed circuit board applications and the results are reported here.

Characterization of Cellulose-laponite composites:

XRD analysis:

XRD diffractograms of the investigated materials are shown in Figure I and compared to the native α-cellulose and laponite powders. The XRD spectrum of cellulose powder shows a broad peak at 2θ = 18.3°, sharp peak at 2θ = 25.9°, and a small peak at 2θ = 40.3°, which could be attributed to the crystallographic planes (-110), (200) and (004) of crystalline cellulose I [23, 24]. The XRD pattern for regenerated from ionic liquid cellulose is different to native cellulose and shows two broad low intensity peaks at 2θ = 12.6 and 24.1°, which correspond to (-110) and (110) crystallographic planes of cellulose II [23, 25]. Thus, the dissolution of cellulose in ionic liquid followed by the regeneration process reduces the crystallinity of cellulose. A similar change in XRD patterns for original and regenerated from ionic liquid celluloses, along with lower degree of polymerisation (DP) values and crystallinity, were observed by Sun *et al.*[25] This is clearly indicating that original crystal structure of cellulose (cellulose-I) is transforming to a distorted crystal structure (cellulose-II) after treated with ILs. XRD analysis showed incorporation of laponite clay within the cellulose matrix, because the characteristic peaks of the clay are visible in the diffractograms of the composites at 2θ = 22.9, 32.3, 40.7 and 71.8 corresponding to (100), (005), (110) and (300) crystal planes [26]. However, there is no remarkable changes in the laponite structure in cellulose-laponite composites.

Thermogravimetric analysis (TGA):

The thermal stability of the prepared cellulose composites was analysed by TGA under air. The initial weight loss observed until 110°C is related to the loss of water from the composites. The weight loss observed in the temperature range from 220-270°C may be due to the oxidation followed by the decomposition of the cellulose unit which are considerably under control by adding a various amount of laponite into the cellulose (see ESI Figure S-I). Thus, the thermal stability was increased by about 17°C while increasing the laponite quantity from 0 to 20 wt% (See ESI, Table S-I). This TGA results suggests that the laponite acts as a heat resistant barrier to protect the cellulose from the thermal oxidative degradation [27]. The weight loss was observed from 330°C is attributed to the thermal-oxidative degradation of cellulose char and

further weight loss under control at higher temperature is based on the weight percentage of laponite residue present in the charred cellulose-laponite composites.

Flame retardancy (FR) test:

Flame retardancy is one of the important parameter for rating the practical application of cellulose based materials for industrial applications. Therefore, we have tested the FR property of the prepared cellulose composites. It can be observed in Figure II that the addition of laponite into the α-cellulose improves the flame retardancy property of the cellulose (flammability property controlled up to 62% with the addition of 20 wt% of laponite into cellulose). This is in good agreement with the above thermal stability study.

Mechanical properties:

In order to study the influence of the clay on mechanical properties of the prepared cellulose composites, static tensile tests were carried out on materials obtained from pure cellulose and cellulose with 5, 10 and 20 wt% of laponite. Both neat cellulose and the composites with 5 and 10 wt% of the clay followed the behaviour of ductile materials, showing well defined elastic region followed by plastic region with increased force loading (Figure III). The sample with 20 wt% of laponite yielded a stress-strain curve of a brittle material. Young's moduli are similar for the neat cellulose material and cellulose modified with 5 and 10 wt% of laponite (Table I), whereas higher loading of laponite of 20 wt%, led to a decrease in Young's modulus by 8 % compared to the neat cellulose. The more profound reduction in the mechanical properties of the materials on the addition of the clay was observed for the ultimate tensile strength and maximum elongation, which gradually reduce with the increase in the clay loading. Thus, the ultimate tensile strength of cellulose material dropped by 24 % (from 60.6 MPa to 45.8 MPa), when 20 wt% of laponite was added to the cellulosic material. As laponite content increased from 0 to 5, 10 and 20 wt% in cellulose, interaction between the fillers (laponite) tend to agglomerates and random distribution of laponite in cellulose composite as visible in the SEM images (Figure IV b -d), act as stress concentrators which may lead to reduction of mechanical properties [28, 29]. Overall, addition of the clay to cellulose makes the material less ductile and more brittle however the influence of the clay on Young's moduli is significant only at high laponite loading of 20 wt%.

SEM analysis

The distribution of the clay within the polymeric matrix, the interaction between them and the mode of fracture were studied by SEM using the fractured specimens after the tensile testing. As it can be seen in Figure IVa, the cross-section of the neat cellulose is smooth and even. The surface is covered with small V-shaped "chevron" markings, some of which expand to craters with particles at the bottom. This pattern is more commonly seen for brittle fractures, however tensile testing of the neat cellulose showed distinctive ductile properties. The observed particles could be undissolved cellulose grains or impurities and work as the crack initiation sites, reducing the strength of the samples. The micrographs of the all cellulose-laponite composites showed the same fracture pattern characteristic of ductile fracture: numerous "dimples" with grains of laponite at the core. It could be noticed that the size of the clay particles varies significantly between 10 – 150 µm (though *the calculated average particle size of laponite was 4-10 µm before being added into cellulose/[emim][OAc] mixture*). Clearly visible voids between the clay grains and the matrix point at weak interaction between the polymers and the particles. This would lead to a significant worsening of mechanical properties, but apparently was compensated by reinforcing properties of the clay because the tensile testing showed a significant decrease in composite strength only at 20 wt% loading of laponite. Deformation, displacement and cracks on the grains of laponite show that the clay filler dissipates stress within the polymeric matrix. It is predicted, that by reducing the size of the used clay particles, which are less prone to damage under increasing stress, and by improving the interaction of them with the matrix *via* a modified preparation method, the mechanical strength of the composites could be significantly improved.

Preparation of hydrophobized cellulose-laponite composites:

In this work, we have used E2CA (1 wt% in toluene solvent) as a monomer for the hydrophobic agent to modify the hydrophilic cellulose into hydrophobic cellulose [30]. The presence of two electron withdrawing groups (cyanide and ester) makes E2CA as a highly active monomer which is required only water vapour present in the atmosphere or hydroxyl group to get polymerised into PECA at room temperature. Therefore, ethylene group (CH_2=CH-R) of E2CA may reacts with hydroxyl group of cellulose and forms ether linkage. The amount of hydrophobic agent was calculated before and after treated with E2CA and the amount of polymerised E2CA present in the cellulose is estimated to be < 1 wt%. The resultant

hydrophobized cellulose composites were subjected into structural (FTIR), morphological (FE-SEM), surface (AFM) and water contact angle measurements.

Attenuated total reflectance-Fourier transform infrared spectroscopy (ATR-FTIR):

The ATR-FTIR spectra of non-hydrophobized and hydrophobized cellulose-laponite composites films with 0 and 20 wt% laponite are shown in ESI Figure S-II. Firstly, there was no characteristic peak of [emim][OAc] (absence of characteristic peaks of [emim] at 1572 & 1404 cm^{-1}) observed in ATR-FTIR which confirms the complete removal of [emim][OAc] from the regenerated cellulose composites (supporting information Fig. S-IIa) [31]. The addition of laponite into the cellulose is reducing the intensity of the FTIR, possibly due to strong interaction between cellulose and laponite (Fig. S-IIc). Also a slightly broader peak in the range from 1070-977 cm^{-1} observed in the cellulose-laponite composite may be due to the contribution from the Si-O-Si stretching of the laponite (976 cm^{-1}, Fig. S-IIb). The hydrophobized cellulose composites (Fig. S-IIb & IIc) show an additional peak at 1750 cm^{-1} which is related to –C=O stretching in the ester group in PECA polymer confirming the coverage of the cellulose surface with the hydrophobic agent [32, 33]. Other characteristics peaks of PECA may be merged with cellulose and laponite peaks.

Contact angle measurements:

The reduction of hydrophilicity of the cellulose-laponite composites was analysed by contact angle (CA) measurement. As shown in the graph (Figure V) the hydrophilicity was decreased as the laponite quantity increased from 0 to 20 wt%. The maximum hydrophilicity reduction was observed at 5 wt% of laponite (CA = >73°). The reason may be due to the surface roughness increased in presence of laponite. However, the hydrophilicity of the cellulose cannot be controlled only by the fillers and required the additional surface modification to reduce the hydrophilicity (CA = > 90°) of the cellulose. The surface of the cellulose composites were modified as mentioned in the experimental section by treating with monomer of the hydrophobic agent E2CA. As shown in the Figure VIa & b, the hydrophilicity of the cellulose (0 wt% laponite) was reduced to two fold from the original value (50° to 112°). Furthermore, the tests on the cellulose composite with 20 wt% laponite also showed the similar kind of hydrophilicity reduction (from 58° to 94°) before and after being treated with the hydrophobic agent (Fig. VIc & d). Therefore, the hydrophilicity of the cellulose composite can be reduced by a simple process with very little amount of hydrophobizing agent (< 1 % wt.).

Atomic force microscope (AFM):

The surface roughness of the cellulose composite with 0 wt% of laponite was measured by AFM. The surface roughness values measured using the described software and it can be noticed that the surface of the hydrophobized cellulose composite with 0 wt% of laponite is rougher (Table S-II, Ra = 103 nm and RMS = 121.2 nm) than non-hydrophobized cellulose composite (Ra = 88.3 nm and RMS = 110.8 nm). The increase of surface roughness is directly related to reduction of hydrophilicity of the regenerated cellulose.

Conductive Ag-ink printing studies:

Here, we use a reactive silver ink, as described in the reported literature [34] to evaluate the effect of the hydrophobic surface treatment. In general, the hydrophobic treatment used in these experiments is effective. This can be seen in Figures VII**;** comparing the hydrophobized surfaces (b, d) with the non-hydrophobized counterparts (a, c) shows that the individual droplets are much more well-defined and circular on the treated substrates. The droplets are much smaller due to higher the contact angle, causing the printed tracks to be thinner overall. However this also means that the tracks are discontinuous, and would require additional passes to effectively fill in the gaps that remain; at higher drop densities the close proximity of adjacent droplets cause them to merge together and form a larger droplet. On the non-hydrophobized surfaces, these larger droplets bleed/spread out more which helps create more continuous tracks, but they are very inconsistent in width. This would require a heated printing platform in order to sinter the droplets quickly and give useful printing speeds. Additionally, the printer needs to be accurate enough to position the droplets in the correct places instead of simply landing on the previous drops.

Droplet sizes are measured by using the area of each droplet in the lines with lowest droplet density, i.e. 5 dpmm, as these are spaced far enough apart to not interfere with adjacent droplets. Table 2 shows the mean droplet areas calculated from measuring 30 droplets from the 5 dpmm line, evaluated with ImageJ software.

Addition of filler had marginal effects on overall print quality. On the non-hydrophobized samples droplet sizes are slightly smaller, whereas they are slightly larger on the hydrophobized samples (with the addition of filler). This could be due to small lumps of filler affecting how the droplets sit and dry on the sample surface; the surface is slightly dimpled as a result, and the droplets no longer lay perfectly flat.

Enzymatic hydrolysis

Cellulose-based composites were subjected to enzymatic hydrolysis and the effect of laponite, polyethyl 2-cyanoacrylate (PECA) and Ag used as conductive ink was studied. Figure VIII showed that laponite did not have an effect on cellulases activity. However, the activity decreased by 70% after the hydrophobic coating with PECA regardless if it was printed with Ag or not. These results suggested that PECA coating worked as a barrier between cellulases and cellulose. Hence, hydrophobized composites were washed with acetone in order to dissolve PECA. In this way, the initial activity was recovered (Figure VIII) in those samples coated with PECA. As Ag ink was printed on PECA layer, acetone not only dissolved PECA but also released most of printed Ag from surface. Thus, Ag might be recovered from the composites. On the contrary, the activity on samples uncoated with the hydrophobic agent but printed with Ag was not recovered. In this samples, Ag remained in the surface and the inhibitory effect of the metal continued.

Conclusions:

A series of cellulose-laponite composite was prepared with various mass ratio of the laponite by a simple dissolution process. The [emim][OAc] was used as the efficient, recoverable and reusable dissolution medium without adding any organic solvent. The addition of laponite into the cellulose is increasing the thermal and flame retardancy properties and somewhat decreasing the mechanical properties of the cellulose making it more brittle. The hydrophilicity of the cellulose composites was reduced by treatment with an efficient hydrophobic agent by a very simple process. Hydrophobic treatments used here have been effective on the cellulose samples, increasing the printing resolution given a set of printing parameters. Additionally, surface roughness has shown to have little to no effect on print quality, which is dominated mainly by the surface hydrophilicity. The enzyme biodegradation studies on the cellulose composites revealed that the coating with the hydrophobic agent diminished substantially the hydrolysis of cellulose by cellulases. In this way, PECA reduced the biodegradability of the obtained composites. However, the followed strategy by washing the coated composites with acetone would trigger the enzymatic degradation at the precise time and also would enable a recovery of Ag from the material. Therefore, the prepared cellulose-laponite composite can be used as a substrate material in advanced biodegradable electronic devices.

Funding: This project work was funded by Engineering and Physical Sciences Research Council (EPSRC) with project reference number: EP/K026380/1, United Kingdom. Dr. Janet L Scott has received this research grant.

Declaration of competing interest
The authors declare that they have no conflict of interest.

CRediT authorship contribution statement
Saravanan Chandrasekaran: Conceptualization, Methodology, Formal Analysis and Investigation, Writing - original draft preparation. **Maria Sotenko:** Formal Analysis and investigation, Writing - Review & Editing. **Alvaro Cruz-Izquierdo:** Formal Analysis and Investigation, Writing - Review & Editing. **Zuhayr Rymansaib:** Formal Analysis and Investigation, Writing - Review & Editing. **Pejman Iravani:** Writing - Review & Editing. **Kerry Kirwan:** Writing - Review & Editing. **Janet L Scott:** Conceptualization, Funding Acquisition, Resources and Supervision.

Acknowledgement:
Authors are gratefully acknowledged the Engineering and Physical Sciences Research Council (EPSRC), United Kingdom for project funding for project CLEVER. Authors thanks to all other project collaborator from Newcastle University, University of Oxford, University of Surrey and Loughborough University for their kind support during the CLEVER project discussion. SC and JLS thanks to University of Bath, Department of Chemical Engineering staff for their great support during the research activities in their lab.

References:

1. Ratajczak K, Stobiecka M (2020) High-performance modified cellulose paper-based biosensors for medical diagnostics and early cancer screening: A concise review. Carbohydr Polym 229:115463. https://doi.org/10.1016/j.carbpol.2019.115463
2. Zhou S, Kong X, Zheng B, et al (2019) Cellulose Nanofiber @ Conductive Metal–Organic Frameworks for High-Performance Flexible Supercapacitors. ACS Nano 13:9578–9586. https://doi.org/10.1021/acsnano.9b04670
3. Gui Z, Zhu H, Gillette E, et al (2013) Natural Cellulose Fiber as Substrate for Supercapacitor. ACS Nano 7:6037–6046. https://doi.org/10.1021/nn401818t
4. Bayer IS, Fragouli D, Attanasio A, et al (2011) Water-Repellent Cellulose Fiber Networks with Multifunctional Properties. ACS Appl Mater Interfaces 3:4024–4031. https://doi.org/10.1021/am200891f
5. Chen C, Hu L (2018) Nanocellulose toward Advanced Energy Storage Devices: Structure and Electrochemistry. Acc Chem Res 51:3154–3165. https://doi.org/10.1021/acs.accounts.8b00391
6. Wang S, Yu Y (2013) Bioactive Bead Type Cellulosic Adsorbent for Blood Purification. In: Cellulose - Medical, Pharmaceutical and Electronic Applications. InTech
7. Baptista A, Ferreira I, Borges J (2013) Cellulose-Based Bioelectronic Devices. In: Cellulose - Medical, Pharmaceutical and Electronic Applications. InTech
8. Shokri J, Adibki K (2013) Application of Cellulose and Cellulose Derivatives in Pharmaceutical Industries. In: Cellulose - Medical, Pharmaceutical and Electronic Applications. InTech
9. Song Z, Xiao H, Zhao Y (2014) Hydrophobic-modified nano-cellulose fiber/PLA biodegradable composites for lowering water vapor transmission rate (WVTR) of paper.

Carbohydr Polym 111:442–448. https://doi.org/10.1016/j.carbpol.2014.04.049
10. Nakashima K, Yamaguchi K, Taniguchi N, et al (2011) Direct bioethanol production from cellulose by the combination of cellulase-displaying yeast and ionic liquid pretreatment. Green Chem 13:2948. https://doi.org/10.1039/c1gc15688h
11. Mascal M, Nikitin EB (2008) Direct, High-Yield Conversion of Cellulose into Biofuel. Angew Chemie Int Ed 47:7924–7926. https://doi.org/10.1002/anie.200801594
12. Jabbour L, Bongiovanni R, Chaussy D, et al (2013) Cellulose-based Li-ion batteries: a review. Cellulose 20:1523–1545. https://doi.org/10.1007/s10570-013-9973-8
13. Rahatekar SS, Rasheed A, Jain R, et al (2009) Solution spinning of cellulose carbon nanotube composites using room temperature ionic liquids. Polymer 50:4577–4583. https://doi.org/10.1016/j.polymer.2009.07.015
14. Liu Y, Wang Y, Nie Y, et al (2019) Preparation of MWCNTs-Graphene-Cellulose Fiber with Ionic Liquids. ACS Sustain Chem Eng 7:20013–20021. https://doi.org/10.1021/acssuschemeng.9b05489
15. Wang W, Nie Y, Liu Y, et al (2017) Preparation of cellulose/multi-walled carbon nanotube composite membranes with enhanced conductive property regulated by ionic liquids. Fibers Polym 18:1780–1789. https://doi.org/10.1007/s12221-017-7298-1
16. Zhang H, Wang ZG, Zhang ZN, et al (2007) Regenerated-Cellulose/Multiwalled-Carbon-Nanotube Composite Fibers with Enhanced Mechanical Properties Prepared with the Ionic Liquid 1-Allyl-3-methylimidazolium Chloride. Adv Mater 19:698–704. https://doi.org/10.1002/adma.200600442
17. Zakrzewska ME, Bogel-Łukasik E, Bogel-Łukasik R (2010) Solubility of Carbohydrates in Ionic Liquids. Energy & Fuels 24:737–745. https://doi.org/10.1021/ef901215m
18. Zavrel M, Bross D, Funke M, et al (2009) High-throughput screening for ionic liquids dissolving (ligno-)cellulose. Bioresour Technol 100:2580–2587. https://doi.org/10.1016/j.biortech.2008.11.052
19. Pinkert A, Marsh KN, Pang S, Staiger MP (2009) Ionic Liquids and Their Interaction with Cellulose. Chem Rev 109:6712–6728. https://doi.org/10.1021/cr9001947
20. Vitz J, Erdmenger T, Haensch C, Schubert US (2009) Extended dissolution studies of cellulose in imidazolium based ionic liquids. Green Chem 11:417. https://doi.org/10.1039/b818061j
21. Swatloski RP, Spear SK, Holbrey JD, Rogers RD (2002) Dissolution of Cellose with Ionic Liquids. J Am Chem Soc 124:4974–4975. https://doi.org/10.1021/ja025790m
22. Ghose TK (1987) Measurement of cellulase activities. Pure Appl Chem 59:257–268. https://doi.org/10.1351/pac198759020257
23. Liu Z, Sun X, Hao M, et al (2015) Preparation and characterization of regenerated cellulose from ionic liquid using different methods. Carbohydr Polym 117:99–105. https://doi.org/10.1016/j.carbpol.2014.09.053
24. Yuan Z, Fan Q, Dai X, et al (2014) Cross-linkage effect of cellulose/laponite hybrids in aqueous dispersions and solid films. Carbohydr Polym 102:431–437. https://doi.org/10.1016/j.carbpol.2013.11.051
25. Pang J, Wu M, Zhang Q, et al (2015) Comparison of physical properties of regenerated cellulose films fabricated with different cellulose feedstocks in ionic liquid. Carbohydr Polym 121:71–78. https://doi.org/10.1016/j.carbpol.2014.11.067
26. Daniel LM, Frost RL, Zhu HY (2008) Edge-modification of laponite with dimethyl-octylmethoxysilane. J Colloid Interface Sci 321:302–309. https://doi.org/10.1016/j.jcis.2008.01.032
27. Cerruti P, Ambrogi V, Postiglione A, et al (2008) Morphological and Thermal Properties of Cellulose−Montmorillonite Nanocomposites. Biomacromolecules 9:3004–3013.

https://doi.org/10.1021/bm8002946
28. Alves L, Ferraz E, Gamelas JAF (2019) Composites of nanofibrillated cellulose with clay minerals: A review. Adv Colloid Interface Sci 272:101994. https://doi.org/10.1016/j.cis.2019.101994
29. Medina L, Nishiyama Y, Daicho K, et al (2019) Nanostructure and Properties of Nacre-Inspired Clay/Cellulose Nanocomposites—Synchrotron X-ray Scattering Analysis. Macromolecules 52:3131–3140. https://doi.org/10.1021/acs.macromol.9b00333
30. Du X, Li JS, Li LX, Levkin PA (2013) Porous poly(2-octyl cyanoacrylate): a facile one-step preparation of superhydrophobic coatings on different substrates. J Mater Chem A 1:1026–1029. https://doi.org/10.1039/C2TA00934J
31. Sundberg J, Toriz G, Gatenholm P (2013) Moisture induced plasticity of amorphous cellulose films from ionic liquid. Polymer 54:6555–6560. https://doi.org/10.1016/j.polymer.2013.10.012
32. Xu J, Zhang L, Chen G (2013) Fabrication of graphene/poly(ethyl 2-cyanoacrylate) composite electrode for amperometric detection in capillary electrophoresis. Sensors Actuators B Chem 182:689–695. https://doi.org/10.1016/j.snb.2013.03.109
33. Han MG, Kim S, Liu SX (2008) Synthesis and degradation behavior of poly(ethyl cyanoacrylate). Polym Degrad Stab 93:1243–1251. https://doi.org/10.1016/j.polymdegradstab.2008.04.012
34. Walker SB, Lewis JA (2012) Reactive Silver Inks for Patterning High-Conductivity Features at Mild Temperatures. J Am Chem Soc 134:1419–1421. https://doi.org/10.1021/ja209267c

Figures and Tables Captions:

Figure I. XRD diffractograms of the studied samples: α-cellulose powder, laponite powder and the prepared cellulose composites with 0, 5, 10 and 20 wt% of laponite.

Figure II: FR property of the cellulose composite with 0, 5, 10 and 20 wt% of laponite.

Figure III. Stress vs. strain curves obtained for the neat cellulose material and modified with 0, 5, 10 and 20 wt% of laponite.

Figure IV. Scanning electron microscope fractography of the cross sections of the following cellulose composites with a) 0 wt% laponite, b) 5 wt% laponite, c) 10 wt% laponite, d) 20 wt% laponite.

Figure V: Surface contact angle measurements of regenerated cellulose composites with 0, 5, 10 and 20 wt% laponite before and after hydrophobizing agent treatment.

Figure VI: Images of surface contact angle measurements of before and after hydrophobized cellulose composites with a, b) 0 wt% and c, d) 20 wt% of laponite.

Figure VII: Printed lines on cellulose samples. a) non-hydrophobized cellulose film, b) hydrophobized cellulose film, c) non-hydrophobized cellulose-20 wt% laponite and d) hydrophobized cellulose – 20 wt% laponite film. Each image shows 3 different drop densities; 15 dpmm (left), 10 dpmm (middle) and 5 dpmm (right). Scale bar 2 mm.

Figure VIII: Cellulases activity (FPU/g) with different cellulose-based composites as substrates.

Figure I:

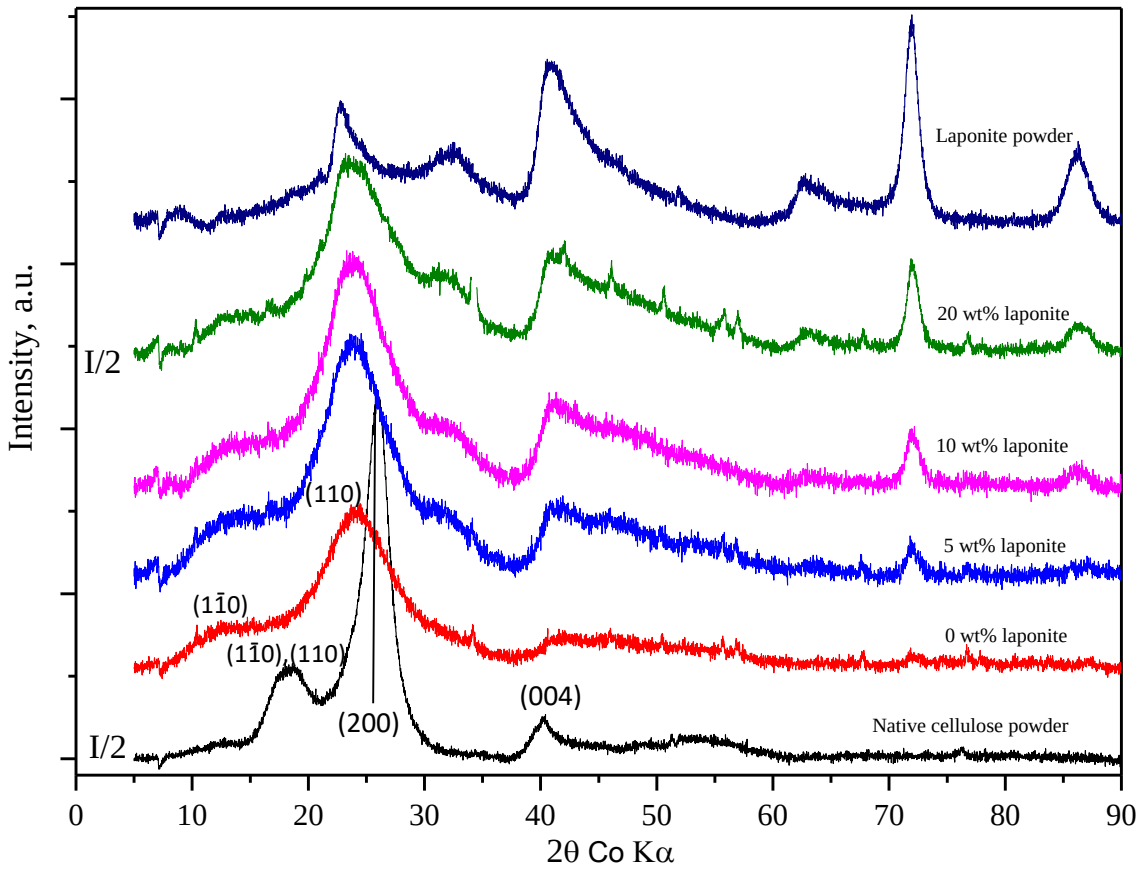

Figure II:

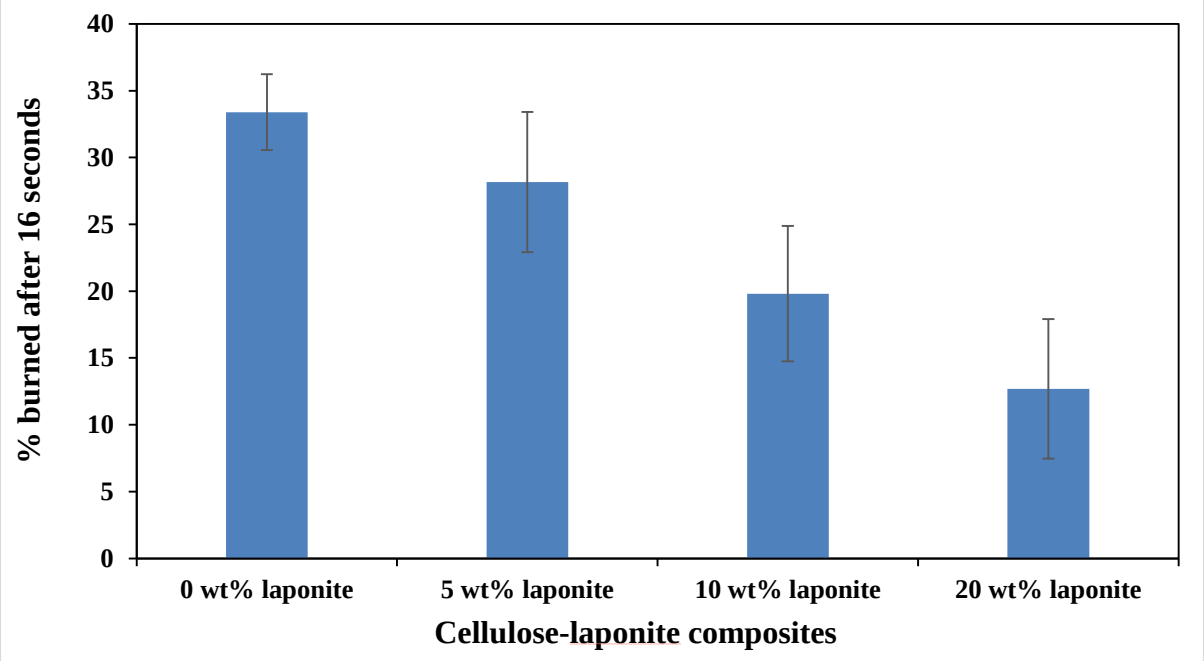

Figure III:

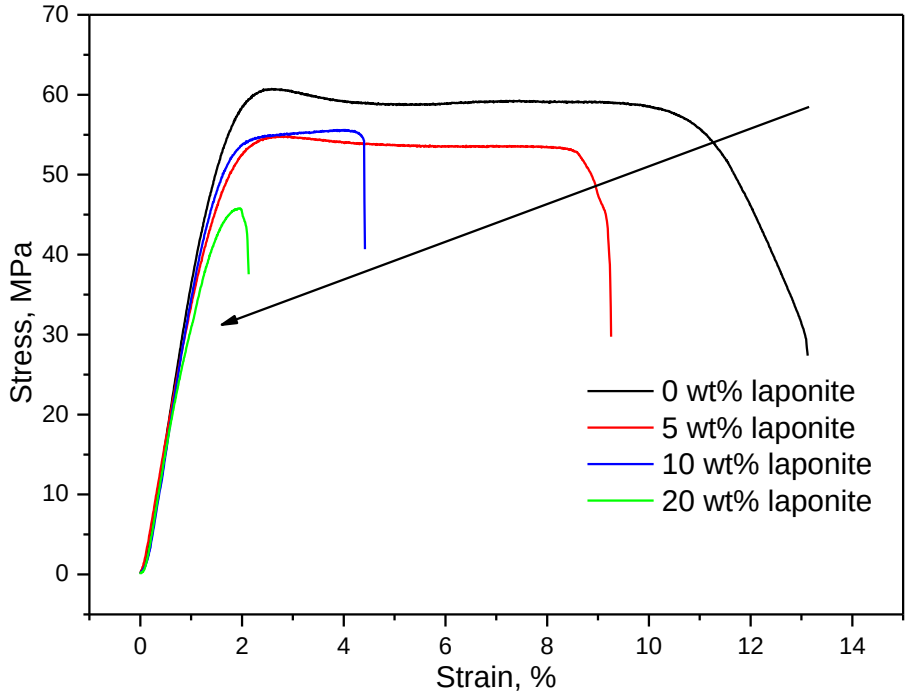

Figure IV:

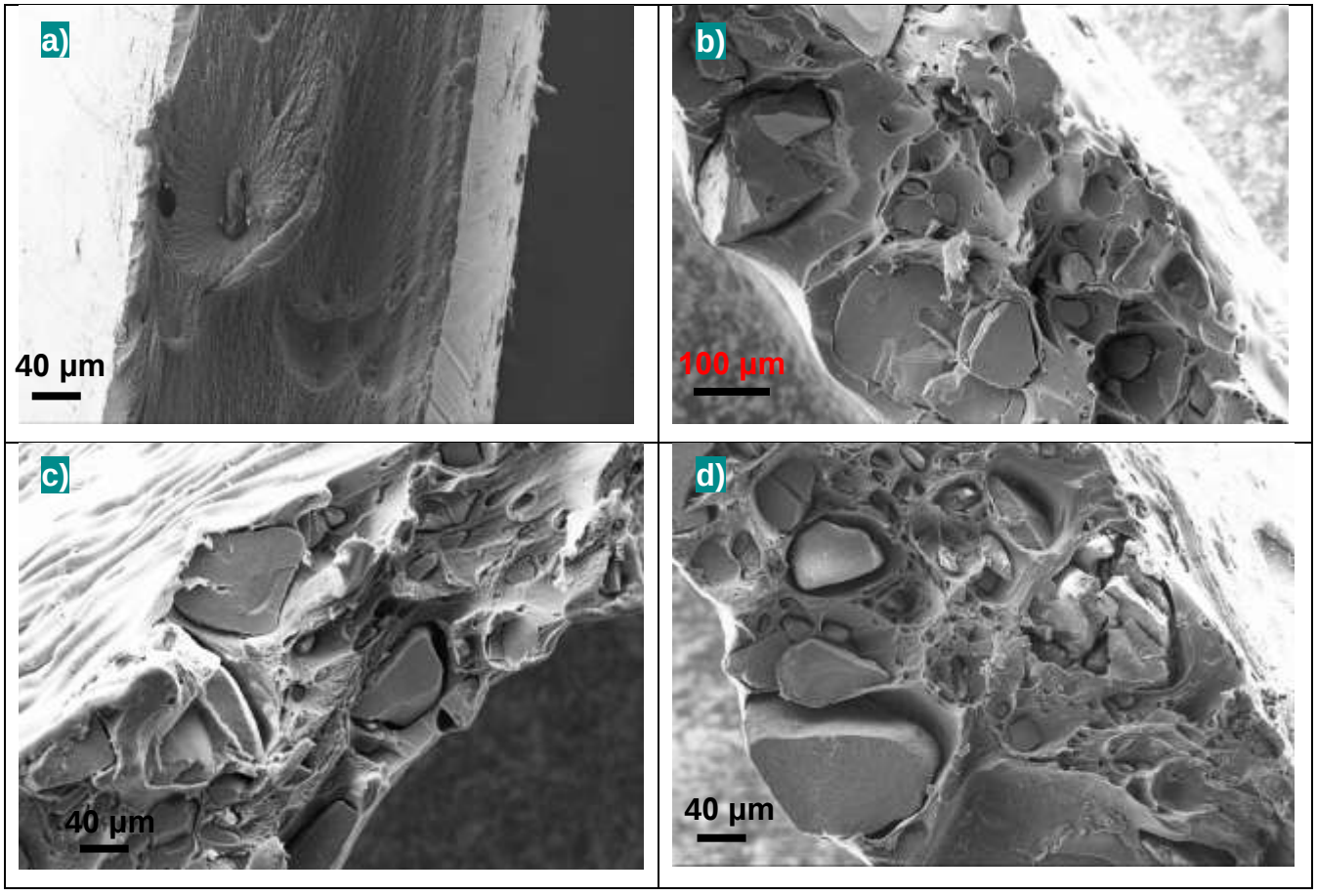

Figure V:

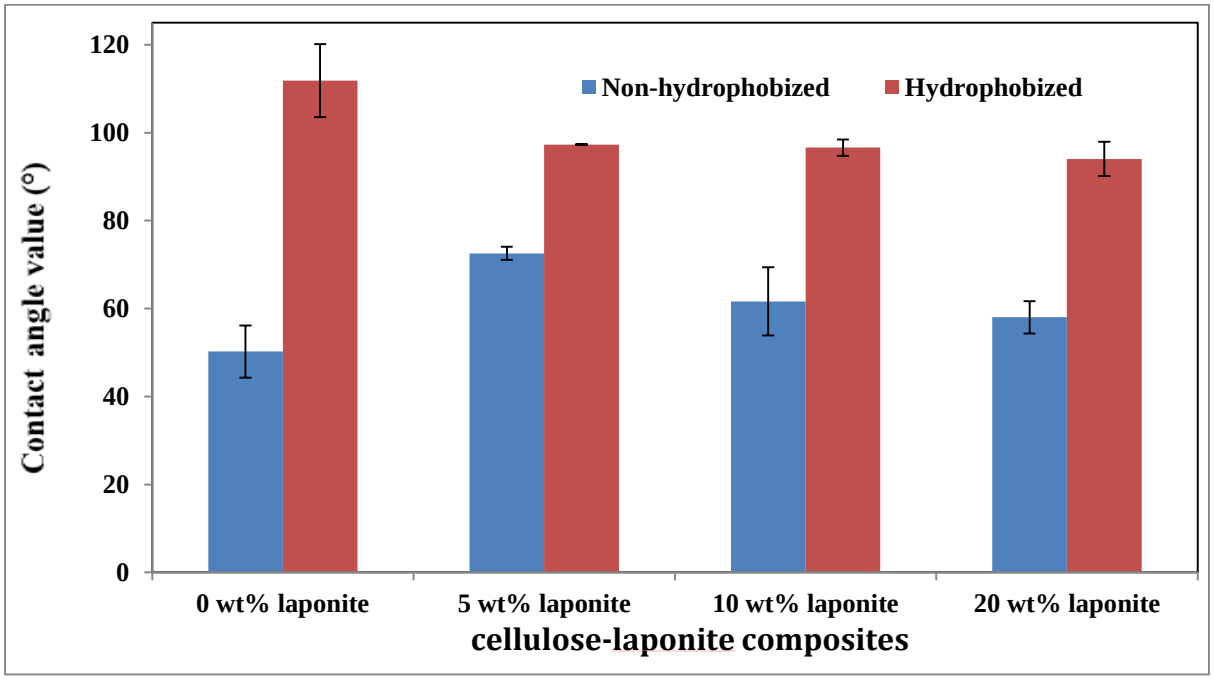

Figure VI:

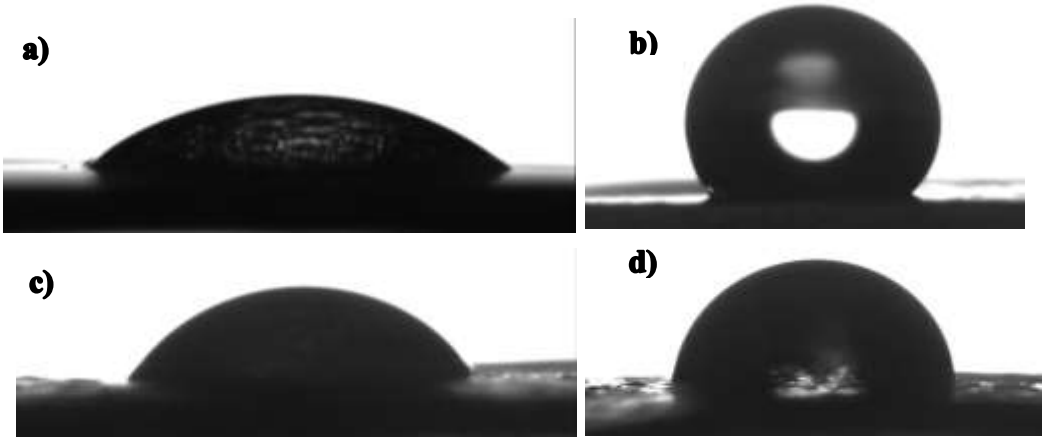

Figure VII:

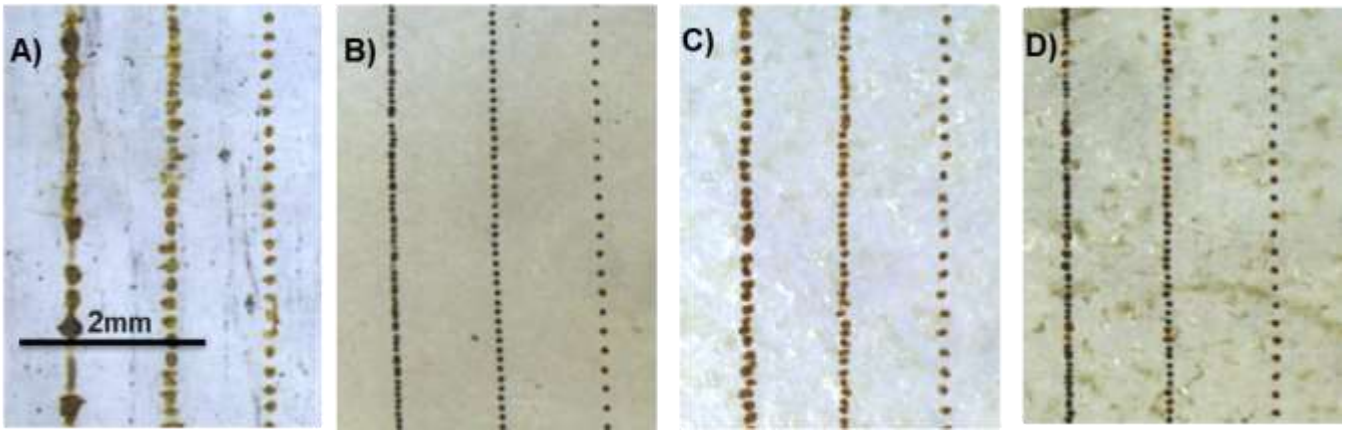

Figure VIII:

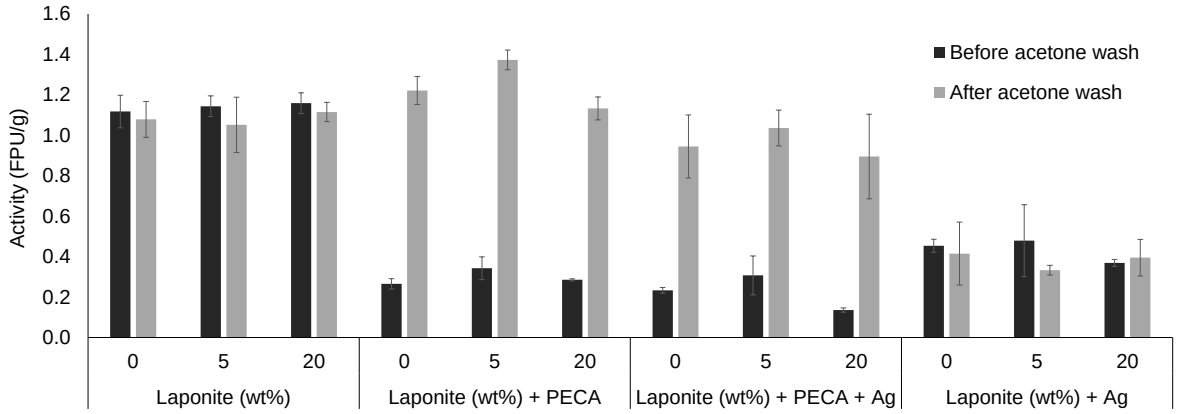

Table I. Young's moduli and ultimate tensile strength for the cellulose composites with different loading of laponite.

Table II: Calculated average droplet diameters (μm) formed on the cellulose samples

Table I.

Sample	**Laponite content, wt%**	**Young's Modulus, MPa**	**Ultimate Tensile Strength, MPa**
Neat Cellulose	0	3964 ± 253	60.6 ± 3.8
Cellulose composites with laponite	5	3820 ± 437	55.8 ± 3.1
	10	3987 ± 319	54.5 ± 1.6
	20	3662 ± 113	45.8 ± 1.9

Table II:

Mean droplet area (μm^2) non-hydrophobized cellulose		**Mean droplet area (μm^2) Hydrophobized cellulose**	
(a) 0 wt% laponite	(c) 20 wt% laponite	(b) 0 wt% laponite	(d) 20 wt% laponite
8550 (SD 1030)	6570 (SD 660)	3760 (SD 430)	4780 (SD 920)

SD = standard deviation

Supporting information

Preparation of printable and biodegradable cellulose-laponite composite for electronic device application

Saravanan Chandrasekaran,*[a,d] Maria Sotenko,[b] Alvaro Cruz-Izquierdo,[a] Zuhayr Rymansaib,[c] Pejman Iravani[c], Kerry Kirwan[b] and Janet L Scott*[a]

[a]Centre for Sustainable Chemical Technologies and Department of Chemistry, University of Bath, Claverton Down, Bath, BA2 7AY, United Kingdom

[b]Warwick Manufacturing Group, International Manufacturing Centre, University of Warwick, Gibbet Hill, Coventry, CV4 7AL, United Kingdom

[c]Department of Mechanical Engineering, University of Bath, Claverton Down, Bath, BA2 7AY, United Kingdom

[d]Department of Chemistry, School of Engineering, Presidency University, Rajanukunte, Itgalpura, Bangalore – 560064, India.

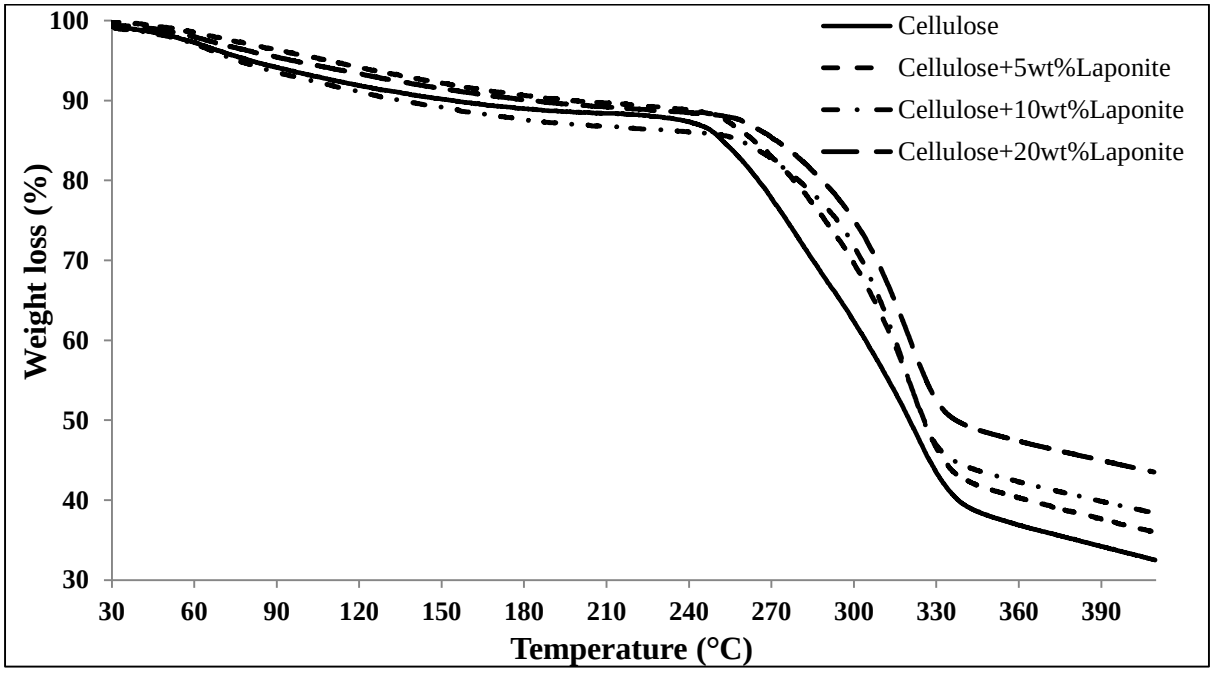

Figure S-I: TGA analysis on cellulose composite with 0, 5, 10, 20 wt% of laponite under air at 5°C/min.

Sl.No	Materials	Degradation temperature (°C)
1	Cellulose with 0wt% Laponite	246
2	Cellulose with 5wt% Laponite	254
3	Cellulose with 10wt% Laponite	260
4	Cellulose with 20wt% Laponite	263

Table S-I: Degradation points of Cellulose composite with 0, 5, 10, 20 wt% of laponite under air at 5°C/min calculated from the TGA.

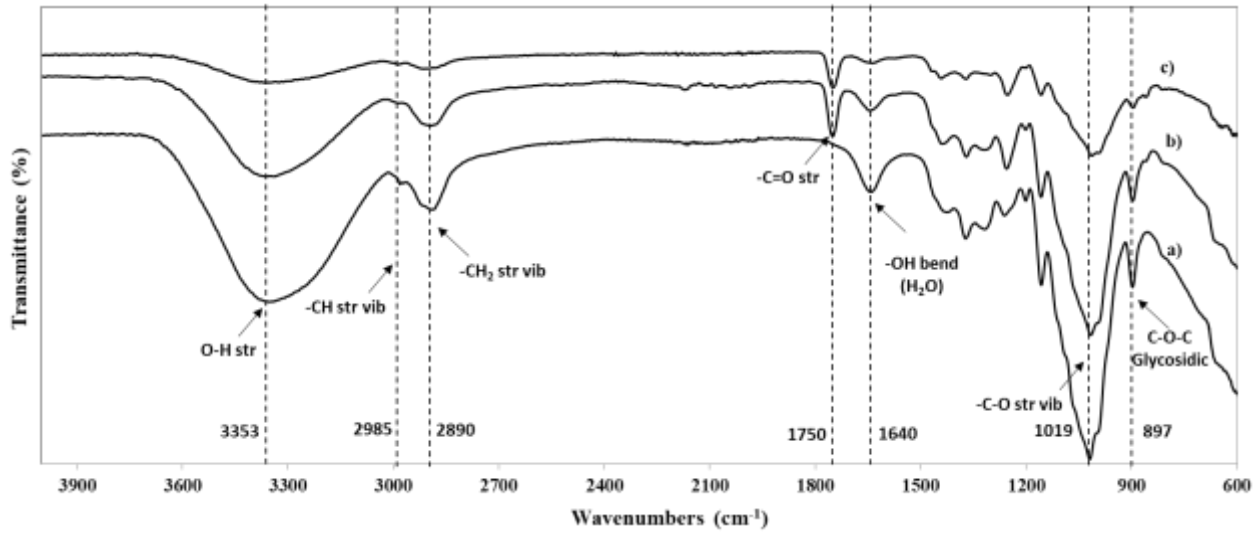

Figure S-II: ATR-FTIR of a) regenerated cellulose, hydrophobized regenerated cellulose composite with b) 0 wt% and c) 20 wt% laponite.

Non-hydrophobized materials	**Hydrophobized materials**
Ra: 88.3 nm Rms: 110.8 nm	Ra: 103.0 nm Rms: 121.2 nm

Table S-II: AFM data obtained from the AFM images of the non-hydrophobized and hydrophobized regenerated Cellulose using Gwyddion software.